



ELSEVIER

Comparative Biochemistry and Physiology Part A 00 (2001) 00–00

CBP

www.elsevier.com/locate/cbpa

# Red muscle function during steady swimming in brook trout, *Salvelinus fontinalis*

S.M. McGlinchey, K.A. Saporetti, J. Forry, J.A. Pohronezny, D.J. Coughlin\*

Department of Biology, Widener University, One University Place, Chester, PA 19013 USA

Received 19 September 2000; received in revised form 14 February 2001; accepted 19 February 2001

## Abstract

Red muscle function during steady swimming in brook trout was studied through both in vivo swimming and in vitro muscle mechanics experiments. In the swimming experiments, red muscle activity was characterized through the use of electromyography and sonomicrometry, allowing the determination of several parameters such as tailbeat frequency, EMG burst duration, muscle length change patterns and relative phase of EMG activity and length change. Brook trout do show some shifts in these variables along their length during steady swimming, but the magnitude of these shifts is relatively small. In the muscle mechanics experiments, the in vivo muscle activity data were used to evaluate patterns of power production by red muscle during swimming. Unlike many fish species, the red muscle along the length of brook trout shows little change in isometric kinetic variables such as relaxation rate and twitch time. Furthermore, there is no rostral–caudal shift in red muscle mass-specific power output during steady swimming. This last result contrasts sharply with rainbow trout and with a variety of other fish species that power steady swimming primarily with the posterior red myotome. © 2001 Published by Elsevier Science Inc.

**Keywords:** EMG; Sonomicrometry; Power output; Muscle physiology; Salmonid; Rainbow trout; Contraction kinetics

## 1. Introduction

Over the last decade, a debate has developed concerning how fish use their red or slow-twitch, aerobic muscle for swimming. The debate has centered on longitudinal variations in power production, with a variety of interpretations on whether the principal source of power during

swimming is the anterior musculature, the posterior musculature or a generalized feature of the full length of the red myotome. To evaluate how the red muscle is used for steady swimming, two types of data are typically needed. First, red muscle activity must be observed in vivo in swimming experiments. Then, the impact of observed muscle activity conditions on power output by muscle must be determined, either through computer modeling or in vitro measurements of force and power output.

Longitudinal variations in the muscle activity during steady swimming contribute to the debate

\* Corresponding author. Tel.: +1-610-499-4025; fax: +1-610-499-4496.

E-mail address: coughlin@pop1.science.widener.edu (D.J. Coughlin).

70

71 on how red muscle is used to power swimming.  
72 For instance, the amplitude of muscle length  
73 change or muscle strain typically increases from  
74 anterior to posterior, while the duration of elec-  
75 trical activity or EMG duty cycle decreases. The  
76 phase of muscle activation also shifts from the  
77 front of the fish to the back. Anterior muscle  
78 typically shows a small phase shift, with red mus-  
79 cle EMG onset time just before the muscle  
80 reaches its peak length and begins shortening. At  
81 more posterior positions, there is a greater phase  
82 shift, with muscle activity occurring earlier and  
83 earlier in each length change cycle. This descrip-  
84 tion of in vivo red muscle activity has been  
85 observed in general in a variety of fishes (Al-  
86 tringham and Ellerby, 1999), including carp (van  
87 Leeuwen et al., 1990), bass (Jayne and Lauder,  
88 1995b), scup (Rome et al., 1993; Coughlin and  
89 Rome, 1996; Swank and Rome, 2000), rainbow  
90 trout (Coughlin, 2000) and mackerel and saithe  
91 (Wardle and Videler, 1993). The magnitude of  
92 variation of these different quantities differs  
93 between species, and some species do not show  
94 all of the above described trends in muscle activ-  
95 ity, such as tuna (Shadwick et al., 1999) and eel  
96 (Gillis, 1998).

97 Data collected from red muscle during  
98 swimming experiments in fishes have been em-  
99 ployed by various researchers examining  
100 rostral–caudal variations in power output during  
101 steady swimming. Using in vivo muscle activity  
102 and contraction kinetics data with various forms  
103 of modeling, van Leeuwen et al. (1990), Wardle  
104 and Videler (1993), van Leeuwen (1995) con-  
105 cluded that mackerel, saithe, and carp power their  
106 steady swimming primarily through the use of the  
107 anterior red musculature. The posterior red mus-  
108 cle was theorized to generate some power for  
109 swimming but also to act as a stiffened rod that  
110 transmitted force from the anterior muscle to the  
111 tail blade (see Wardle et al., 1995; Altringham  
112 and Ellerby, 1999). Using a modeling technique  
113 that employed in vivo muscle activity data and  
114 contraction kinetics to estimate power produc-  
115 tion, Shadwick et al. (1998) suggested that mack-  
116 erel power steady swimming along the length of  
117 the fish.

118 Using the workloop technique with in vitro  
119 muscle bundles, Rome et al. (1993) reported that  
120 in scup, the power for swimming is generated by  
121 the posterior musculature. The anterior muscula-  
ture generated much less power for swimming

122 and alternatively may act to stabilize the head.  
123 Coughlin (2000) found the same general result in  
124 largemouth bass and in a rainbow trout smolts.  
125 Hammond et al. (1998), also using the workloop  
126 technique, suggested that power production is a  
127 generalized feature of the entire myotome in  
128 large, adult rainbow trout.  
129

The above discussion refers generally to longi-  
130 tudinal variation in mass-specific power output.  
131 Such data permit evaluation of the interaction of  
132 rostral–caudal variations in the contraction kinet-  
133 ics of muscle with activation conditions of the  
134 muscle. To make specific conclusions about power  
135 production in absolute terms, data are needed on  
136 the cross-section and mass of muscle at different  
137 longitudinal positions. Previous work on scup  
138 (Zhang et al., 1996; Coughlin and Rome, 1996)  
139 showed that the longitudinal variation in mass-  
140 specific power output by red muscle during  
141 swimming (posterior muscle produces 10-fold  
142 more power than anterior) is magnified by a  
143 skewed distribution of the red muscle. More mus-  
144 cle is found in the posterior red myotome, accen-  
145 tuating the higher power output of the posterior  
146 half of scup during steady swimming. More recent  
147 work has addressed the variation in red muscle  
148 cross-section in a variety of fish and showed that  
149 the largest cross-section of red muscle is found  
150 more anteriorly in thunniform or stiff-bodied,  
151 tuna-like swimmers (Ellerby et al., 2000).  
152

A general conclusion from the above work is  
153 that there is variation in how the red myotomal  
154 muscle is used to power steady swimming in dif-  
155 ferent fish. Longitudinal variations in the muscle  
156 activity conditions combined with variation in the  
157 contractile properties of red muscle (both along  
158 the length of a fish and between fish species)  
159 contribute to a great diversity of solutions to the  
160 problem of using the axial muscle to generate  
161 forward thrust.  
162

In the present study, we used the two-step  
163 technique described above to examine red muscle  
164 function in swimming brook trout, *Salvelinus*  
165 *fontinalis*. Two previous projects on another sal-  
166 monid, rainbow trout, have suggested different  
167 patterns of power production between large juve-  
168 nile smolts (Coughlin, 2000) and adults (Ham-  
169 mond et al., 1998). We used adult brook trout,  
170 which were similar in size to the rainbow trout  
171 smolts used in the previous study, to see if the  
172 two species of trout show the same red muscle  
173 function during steady swimming. We predicted

174 that the brook trout will generate the majority of  
175 power for steady swimming from the posterior red  
176 myostome, but that the ratio of mass-specific  
177 power output of the posterior relative to anterior  
178 muscle will be relatively low ( $\sim 2$ ) as observed in  
179 rainbow trout (Coughlin, 2000).  
180

## 181 2. Materials and methods

### 182 2.1. Experimental animals

183  
184 The experimental animals employed in these  
185 experiments were brook trout, *Salvelinus fontinalis*.  
186 They were obtained from the Huntsdale  
187 Fish Culture Station (Carlisle, Pennsylvania, USA)  
188 of the Fish and Boat Commission of the Com-  
189 monwealth of Pennsylvania. They were housed in  
190 a recirculating aquarium system that was main-  
191 tained at 10°C. The brook trout were raised on a  
192 diet of Zeigler Trout Grower. A total of 11 fish  
193 were used for the swimming experiments, with a  
194 mean ( $\pm$ S.D.) total length of  $20.8 \pm 1.7$  cm and a  
195 mean mass of  $102.1 \pm 26.8$  g. Six fish were used  
196 for the muscle mechanics experiments, with a  
197 mean total length of  $23.8 \pm 1.5$  cm and a mean  
198 mass of  $141.8 \pm 39.7$  g. The Widener University  
199 Institutional Animal Care and Use Committee  
200 reviewed the handling of the animals in accor-  
201 dance with the National Research Council's Guide  
202 for the Care and Use of Laboratory Animals.  
203  
204

### 205 2.2. Swimming experiments

206  
207 Muscle activity during steady swimming in  
208 brook trout was characterized in vivo using elec-  
209 tromyography and sonomicrometry. Physiological  
210 recordings for each fish were made from red  
211 muscle at two out of three longitudinal positions  
212 along the length of the body. The positions are  
213 Anterior (ANT), Middle (MID) and Posterior  
214 (POST), which were, respectively, 35, 55 and 75%  
215 of the total length of the fish. Another EMG  
216 electrode was placed in each fish at the MID  
217 position to measure white muscle recruitment  
218 during higher swimming speeds. Using a hy-  
219 podermic needle, twisted wire electrodes  
220 (MedWire) were placed in the red muscle at each  
221 position. Amplifiers (Grass P511) were used to  
222 filter the EMG signals. The gain on the amplifiers  
223 was typically 20–50 k with a band pass filter of  
224 100–1000 Hz. Sonomicrometry crystals (Triton

225 Technology) were inserted on either side of the  
226 EMG electrode; the crystals were typically 5–6  
227 mm apart. Muscle length change signals were  
228 collected using a sonomicrometer (Triton Tech-  
229 nology Model 120). Muscle activity was recorded  
230 from brook trout swimming  $2.0$ – $5.0$  BL  $s^{-1}$  (in  
231 steps of  $0.5$  BL  $s^{-1}$ ). The order of swimming  
232 speeds was randomized. Fish swam in a re-  
233 circulating flow chamber. The temperature-con-  
234 trolled flume has a 0.40-m long test section of  
235 0.15 m internal diameter clear acrylic pipe. A  
236 calibrated DC motor permitted speeds of  $0.10$ – $1$   
237  $m s^{-1}$ .  
238

239 Sonomicrometry and EMG signals were col-  
240 lected using a PC and a Keithley-Metrabyte DAS-  
241 1601 input/output board. Analysis of the signals  
242 led to the definition of the four parameters that  
243 describe muscle activity at each longitudinal posi-  
244 tion for each swimming speed. At a given  
245 swimming speed, tailbeat frequency was deter-  
246 mined. For each position, the duty cycle of the  
247 EMG activity was the length of an EMG burst  
248 expressed as a proportion of the tailbeat period.  
249 EMG activity was analyzed using custom soft-  
250 ware. Onset and offset times of an EMG burst  
251 were determined visually by graphing short sec-  
252 tions of the computer file. Onset times were usu-  
253 ally obvious, with sharp increases in the ampli-  
254 tude of the EMG signal (see Fig. 3). For offset  
255 times, anterior muscle typically displayed a dis-  
256 crete end to EMG activity as well, while posterior  
257 muscle EMG recordings would commonly have  
258 low frequency oscillations at the end of the EMG  
259 burst. Offset times were carefully determined by  
260 identifying the end of the high frequency EMG  
261 signal from the low frequency motion artifact.

262 The muscle length change was analyzed for  
263 strain, the percent length change of a muscle  
264 during each tailbeat cycle. A comparison of EMG  
265 and sonomicrometry signals determined phase.  
266 The phase is the relative timing of the onset of  
267 EMG activity to the muscle's peak length during  
268 one tail beat period. If the phase is negative,  
269 EMG activity begins before muscle shortening,  
270 while zero phase indicates that the onset of EMG  
271 activity and of muscle shortening occurred at the  
272 same time. Phase was expressed as a proportion  
273 of tailbeat period. From the sonomicrometry  
274 records, body curvature ( $\lambda_B$ ) could be calculated.  
275 Higher values of  $\lambda_B$ , the wavelength of body  
276 curvature in units of body length, indicate less  
body curvature during swimming, and  $\lambda_B$  is calcu-

lated as mechanical wave speed divided by tail-beat frequency. Mechanical wave speed was found through the sonomicrometry signal by determining the transit time of the peak in muscle length progressing from anterior to posterior. The maximum steady swimming speed was defined as the highest speed at which no white muscle recruitment was detected.

### 2.3. Muscle mechanics experiments

After the *in vivo* experiments were performed and the electromyography and sonomicrometry data were collected, *in vitro* muscle mechanics experiments were carried out for four muscle bundles from each longitudinal position. Fish were sacrificed by transection and pith. Live red muscle was dissected from longitudinal bands that run along the mid line of the fish. To expose this region, the fish were scaled and 0.5 mm strips were extracted just above and below the lateral line. The red muscle bundles were taken from the three positions in strips that were each approximately 20% of the total body length. For the mechanics experiments, the ANT position was 0.25–0.45 L, the MID 0.45–0.65 L, and the POST 0.65–0.85 L. Using muscle bundles from a short range of body positions has been used previously in several fish species, such as scup (Rome et al., 1993; Coughlin and Rome, 1996) and rainbow trout and largemouth bass (Coughlin, 2000), to demonstrate longitudinal variations in contraction kinetics.

Individual muscle strips were then reduced to a single myotome by dissection through the use of a stereomicroscope. The red muscle bundles were kept in a physiological saline solution at 10°C (Altringham and Johnston, 1990). The red muscle bundles from the brook trout for the ANT position had an average length of  $2.963 \pm 0.1789$  mm, for the MID position it was  $3.179 \pm 0.2276$  mm and for the POST position it was  $2.513 \pm 0.1563$  mm. The average area for the ANT position was  $0.2669 \pm 0.0643$  mm<sup>2</sup>, for the MID it was  $0.4117 \pm 0.1615$  mm<sup>2</sup>, and for the POST it was  $0.4010 \pm 0.1342$  mm<sup>2</sup>. The smaller cross-section of anterior muscle bundles reflects the lower overall red muscle cross-section in the anterior myotome. The muscle bundles were tied into a muscle mechanics apparatus via 9-0 gauge silk thread. Connective tissue, at one end of the red muscle bundle was secured to a stainless steel hook at-

tached to a servosystem (Cambridge Technology 300s). The other end of the muscle bundle was tied to a stainless steel hook that connected to a load cell (Entran, 2–20 g). The temperature in this muscle mechanics apparatus was maintained at 10°C. All data collection as well as experimental control was carried out using a PC, I/O board, and custom software.

Isometric contractions were performed on the muscle bundles. Stimulation conditions, including muscle length, total stimulus duration, pulse frequency and pulse amplitude were optimized to give maximum tetanic force output. Optimized conditions were typically a 200-ms stimulus composed of 3.0 ms pulses at a frequency of 125 Hz. Stimulation for isometric twitch contractions was typically a 3.0-ms pulse. The maximal tetanus and twitch forces were determined, and the force traces were analyzed for activation time, relaxation time, and twitch time. Activation time is defined as the time from 10 to 90% of peak isometric stress. Relaxation time is from 90 to 10% of peak isometric stress. Lastly, twitch time is from the onset of the EMG, or stimulus, to 90% of the relaxation (10% of peak twitch stress left).

Workloop experiments (Josephson, 1985) were then used to characterize work production and power output by muscle bundles. During oscillatory activity the muscle shortens with high force and is lengthened with low force. Positive work is done by the muscle during shortening and is the product of muscle length change and force level during the shortening phase of the cycle. Negative work is done by the servomotor on the muscle and is a product of muscle length change and force level during the lengthening phase of the cycle. The difference between negative and positive work of one oscillatory cycle corresponds to the area of the work loop, which is the net work/oscillatory cycle. Power is the product of net work/oscillatory cycle and oscillation frequency. Power production was described in mass-specific terms, by dividing the product of work/oscillatory cycle and the oscillation frequency by the mass of the muscle bundle.

Maximum power output and the optimum oscillation frequency for muscle bundles were found by optimizing stimulation conditions for a range of frequencies (2–5 Hz). At a given frequency, the best set of conditions of strain, duty cycle and stimulus phase were optimized to find the maxi-

381 mum power output. A modified triangle wave  
382 with smoothed peaks was employed in this man- 433  
383 ner to ensure that there were no abrupt changes 434  
384 in length. Waveforms observed in the muscula- 435  
385 ture of swimming fish vary between sine and 436  
386 triangle wave. The selection of one or the other 437  
387 of these waveforms for workloop experiments for 438  
388 symmetrical length change patterns will affect the 439  
389 absolute magnitude of power production, but will 440  
390 not affect the relative power output of muscle 441  
391 being stimulated with different activation condi- 442  
392 tions (Coughlin et al., unpublished data). The 443  
393 frequency that yielded the maximum oscillatory 444  
394 power output ( $W_{\max}$ ) was known as the optimal 445  
395 oscillatory frequency ( $F_{\text{opt}}$ ). To control for muscle 446  
396 fatigue, workloops that generated maximum 447  
397 power at a given frequency were consecutively 448  
398 interspersed with trials for  $W_{\max}$  at the optimal 449  
400 frequency.

401 In vitro optimized workloops were used to esti- 450  
402 mate in vivo power production. The conditions 451  
403 that were recorded during the in vivo swimming 452  
404 experiments became the activation conditions for 453  
405 the in vitro workloops. Red muscle bundles from 454  
406 a given position were subjected to the conditions 455  
407 specified at that position for several swimming 456  
408 speeds (2, 3 and 4 BL  $s^{-1}$ ). Work production and 457  
409 power output were measured at each of the 458  
410 swimming speeds using two sets of muscle strains. 459  
411 One set, termed ‘observed strains’, represented 460  
412 the measurements actually made in brook trout 461  
413 and were  $\sim 2$ ,  $\sim 2.5$  and  $\sim 3.5\%$  for anterior, 462  
414 middle and posterior positions. Since the strains 463  
415 observed previously in rainbow trout were con- 464  
416 siderably longer (3, 4 and 5% for the three posi- 465  
417 tions, Coughlin, 2000), a second set of muscle 466  
418 strains based on the rainbow trout data was used 467  
419 and was termed ‘long strains’. This was done to 468  
420 facilitate a comparison between the two species, 469  
421 insuring that differences in the patterns of mass- 470  
422 specific power output were not simply due to 471  
423 differences in muscle strain. 472

424 At the end of all muscle mechanics experi- 473  
425 ments, the muscle bundles were stained for 1 h in 474  
426 Trypan Blue to mark dead tissue. The bundles 475  
427 were then embedded in gelatin, frozen with liquid 476  
428 nitrogen and sectioned at 12  $\mu\text{m}$ . The sections 477  
429 were mounted on slides and stained with succinic 478  
430 dehydrogenase (SDH) for mitochondrial content. 479  
431 Dark blue stained areas were dead tissue, while 480  
432 dark brown corresponded to aerobic muscle fibers. 481  
The area of all live muscle fibers was determined 482  
483

through the use of image analysis software (Opti- 433  
434 mas) after the muscle bundle slides had been 435  
436 digitized. Bundles typically were composed of > 437  
438 90% aerobic muscle fibers. Since salmonid muscle 439  
439 bundles typically contain approximately 30% con- 440  
440 nective tissue (unpublished data), live fiber area 441  
441 of the bundle was found by multiplying the mea- 442  
442 sured area by 0.7. Live fiber mass was estimated 443  
443 by multiplying live fiber area by the muscle bun- 444  
444 dle length and then multiplying by 1.05 to com- 445  
445 pensate for the slightly higher density of muscle 446  
446 mass relative to water. This approach has been 447  
447 used previously (Rome et al., 1993). 448

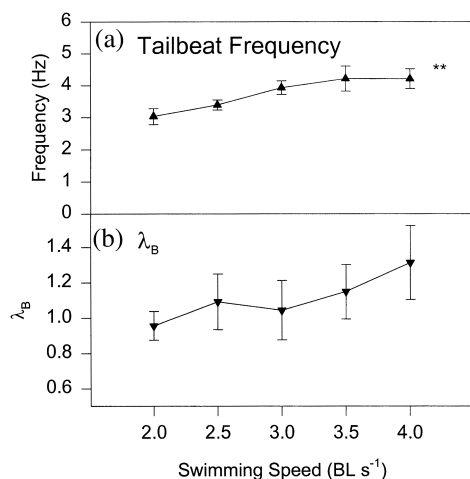
#### 2.4. Distribution of red muscle 449

450 To permit evaluation of how variations in the 451  
451 distribution of red muscle mass affect patterns of 452  
452 power production in absolute terms (as opposed 453  
453 to mass-specific terms), red muscle area was de- 454  
454 termined grossly at seven longitudinal positions 455  
455 (0.25, 0.35, 0.45, 0.55, 0.65, 0.75 and 0.85 TL) in a 456  
456 single brook trout (TL = 23.9 cm). The techniques 457  
457 of Ellerby et al. (2000) were employed. Muscle 458  
458 cross-sections were photographed digitally using 459  
459 an Olympus CZ2100 camera, and the area of the 460  
460 red muscle for each position was determined us- 461  
461 ing Optimas. In addition, previously unpublished 462  
462 data on red muscle area of rainbow trout are 463  
463 presented. These data were collected by section- 464  
464 ing red muscle steaks from six longitudinal posi- 465  
465 tions (0.35, 0.45, 0.55, 0.65, 0.75 and 0.85 TL), 466  
466 staining with SDH, recording digital images of the 467  
467 slides using an Olympus stereomicroscope and 468  
468 determining area at each position using Optimas, 469  
469 similar to the techniques of Zhang et al. (1995). 470  
470 Three to four sections were examined per longi- 471  
471 tudinal position, from a total of six rainbow trout 472  
472 (TL ranges from 12 to 20 cm). 473

### 3. Results 474

#### 3.1. Swimming experiments 475

476  
477  
478 Electromyography and sonomicrometry were 479  
479 used to characterize red muscle activity during 480  
480 steady swimming in brook trout. For most fish 481  
481 steady swimming occurred over a range of speeds 482  
482 from 2.0 to 4.0 BL  $s^{-1}$ . At lower speeds, swimming 483  
483 was generally unpredictable. The mean ( $\pm$  S.E.) 484  
484 maximum steady swimming speed was  $3.9 \pm 0.2$



484

485 Fig. 1. Tailbeat frequency (a) and wavelength of body curva-  
 486 ture (b) for steadily swimming brook trout (mean ± S.E.).  
 487 Data are for 6–11 fish per swimming speed. Both tailbeat  
 488 frequency and the wavelength of body curvature (λ<sub>B</sub>) in-  
 489 creased with swimming speed, although only for tailbeat fre-  
 quency was this trend statistically significant ( $P < 0.01$ ).

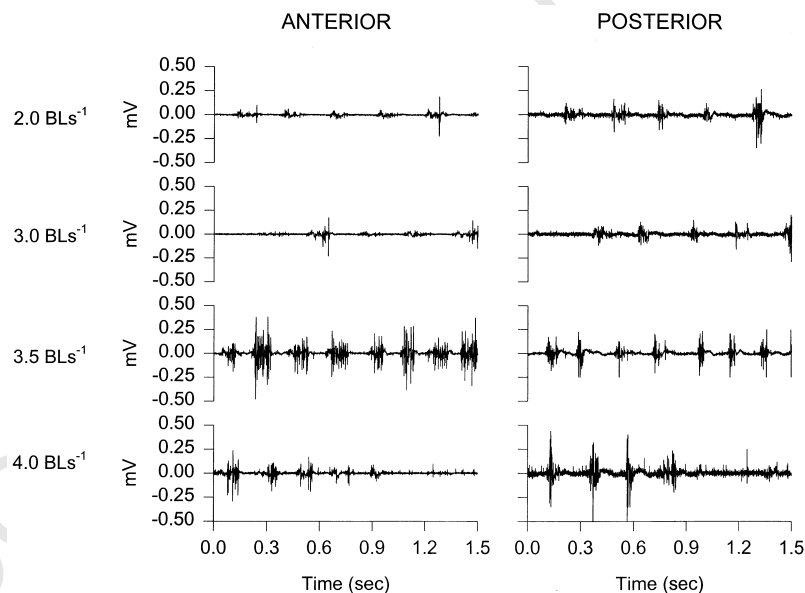
490

491 BL s<sup>-1</sup>. At speeds greater than 4.0 BL s<sup>-1</sup>, most  
 492 fish used a burst and coast swimming behavior.  
 493 Therefore, data from these higher speeds are not  
 494 presented. There was a significant increase in  
 495 tailbeat frequency with swimming speed, ranging  
 from ~ 3.0 Hz at low steady swimming speeds to

> 4 Hz at higher speeds (Fig. 1a). Over the same  
 range of swimming speeds, body curvature during  
 swimming decreased with increasing speeds (Fig.  
 1b). Across the range of steady swimming speeds,  
 λ<sub>B</sub> increased from 1.0 to 1.25 at higher speeds,  
 but this trend was not statistically significant.

Examination of sample EMG data shows a  
 general trend of later recruitment of anterior red  
 muscle relative to posterior muscle (Fig. 2). At  
 low speeds, red muscle activity was primarily de-  
 tected in the posterior myotome, as previously  
 observed in eel and scup (Gillis, 1998; Coughlin  
 and Rome, 1999). Anterior red muscle was re-  
 cruited more intensely at higher steady swimming  
 speeds. For instance, there is a substantial jump  
 in recruitment intensity for the anterior muscle at  
 2.0 vs. 3.0 BL s<sup>-1</sup>, while the increase in recruit-  
 ment intensity across those speeds for the poste-  
 rior muscle is relatively slight (Fig. 2). Examina-  
 tion of sample EMG and length change data  
 reveal that the anterior muscle had a longer duty  
 cycle (EMG burst duration) and a shorter strain  
 (amplitude of muscle length change) than the  
 posterior muscle, but the differences were rela-  
 tively small (Fig. 3).

For duty cycle, phase and strain, multiway  
 ANOVAs were carried out for the two indepen-  
 dent variables: longitudinal position and



524

525 Fig. 2. Sample electromyograms from the anterior and posterior positions of a brook trout at several steady swimming speeds. At the  
 526 lower speeds, the intensity of recruitment of the anterior position was typically much lower than at more posterior positions. In this  
 527 example, recruitment of the anterior myotome dramatically increased at 3.5 BL s<sup>-1</sup> and higher swimming speeds. For this individual,  
 swimming at 4.0 BL s<sup>-1</sup> involved an unsteady, burst and coast behavior.

496

497

498

499

500

501

502

503

504

505

506

507

508

509

510

511

512

513

514

515

516

517

518

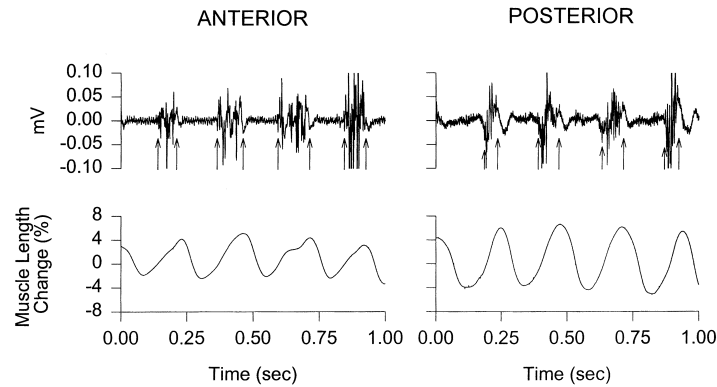
519

520

521

522

523



528 Fig. 3. Electromyogram and muscle length change waveforms for the anterior and posterior positions for a brook trout swimming at 3.0  
 530  $\text{BL s}^{-1}$ . Duration of EMG bursts (duty cycle) was slightly longer in the anterior than the posterior, and the amplitude of muscle length  
 531 change (strain) was longer in the posterior. The representative muscle length graphs shown here were relatively long (2.6% strain for  
 532 anterior and 4.9% strain for posterior) compared to the mean values (see Fig. 4c), but the ratio of the two was similar to the mean  
 533 ratio. These traces were selected to emphasize the modest differences in red muscle kinematics observed in the anterior vs. posterior  
 534 myotome, as opposed to more dramatic differences observed previously in scup and rainbow trout. Arrows mark the approximate onset  
 and offset times of each EMG burst to demonstrate the analysis technique.

535

536 swimming speed. The longitudinal position did  
 537 statistically affect duty cycle, phase and strain  
 538 (Fig. 4). For the duty cycle, there was a significant  
 539 decrease in duty cycle from anterior to posterior  
 540 (Multiway ANOVA,  $P = 0.024$ ). However, there  
 541 was no effect of speed on duty cycle (Multiway  
 542 ANOVA,  $P = 0.051$ ). Furthermore, analysis of in-  
 543 dividual swimming speeds found no single speed  
 544 where position affected duty cycle (ANOVA,  $P >$   
 545  $0.05$  for all speeds). Similar results were observed  
 546 for the phase of muscle activity. There was a  
 547 significant negative shift in the phase from ante-  
 548 rior to posterior (Multiway ANOVA,  $P = 0.002$ ).  
 549 However, there was no effect of speed on phase  
 550 (Multiway ANOVA,  $P = 0.338$ ). Again, analysis of  
 551 individual swimming speeds found no single speed  
 552 where position affected phase (ANOVA,  $P >$   
 553  $0.05$  for all speeds). Lastly, there was a significant  
 554 increase in strain from anterior to posterior (Mul-  
 555 tiway ANOVA,  $P < 0.001$ ). As with the other  
 556 variables, there was no effect of speed on strain  
 557 (Multiway ANOVA,  $P = 0.690$ ). At two individual  
 558 speeds, 3.5 and 4.0  $\text{BL s}^{-1}$ , position did affect  
 559 strain. At those speeds, longitudinal position on  
 560 the body had a significant effect on strain  
 561 (ANOVA,  $P = 0.029$  for 3.5  $\text{BL s}^{-1}$ ,  $P < 0.001$  for  
 562 4.0  $\text{BL s}^{-1}$ ,  $P > 0.05$  for all other speeds).

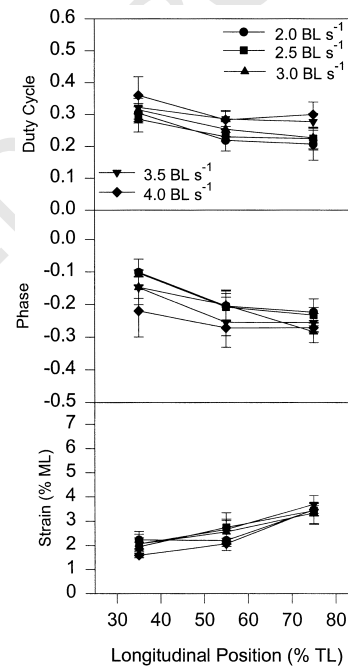
### 564 3.2. Muscle mechanics

565

From the isometric contraction kinetics experi-

566

ments, none of the contraction kinetics variables 567  
 differed with longitudinal position on the fish. 568  
 Activation time did not vary with longitudinal 569  
 position (ANOVA,  $P = 0.717$ ; Fig. 5a). The mean



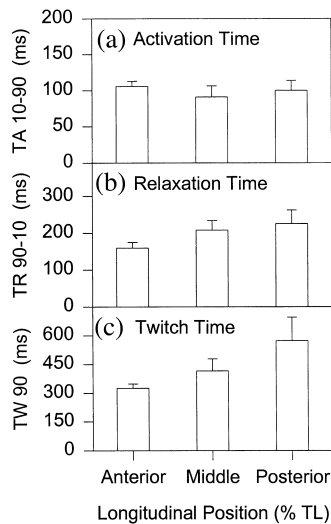
570 Fig. 4. Red muscle activity conditions for three longitudinal 571  
 positions for brook trout swimming across a range of length 572  
 specific swimming speeds (mean  $\pm$  S.E.). Each point is a mean 573  
 ( $\pm$  S.E.) for 4–6 data points. Duty cycle (a) decreases, 574  
 phase (b) shifts more negative and muscle strain (c) increases from 575  
 anterior to posterior.

576

577 ( $\pm$ S.E.) activation time for all positions was 98.8  
 578  $\pm$  6.8 ms. Relaxation time did not differ significantly  
 579 with position (ANOVA,  $P = 0.266$ , Fig. 5b).  
 580 The mean relaxation time for all positions was  
 581  $197.6 \pm 16.6$  ms. Twitch time did not differ across  
 582 the length of the fish as well (ANOVA,  $P = 0.224$ ;  
 583 Fig. 5c). The mean twitch time was  $426.3 \pm 49.2$   
 584 ms for all positions. Longitudinal position also did  
 585 not significantly affect the force generation ( $F =$   
 586  $0.382$ ,  $P = 0.693$ , Fig. 6a). The mean isometric  
 587 tetanic stress generated by a red muscle bundle in  
 588 brook trout was  $149.5 \pm 15.0$  kNm $^{-2}$ .

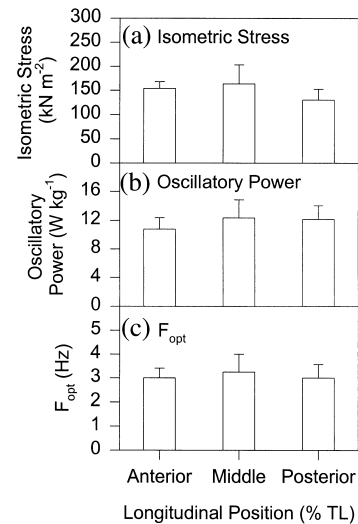
589 Activity conditions were optimized to produce  
 590 maximum oscillatory power.  $F_{opt}$  was not affected  
 591 by longitudinal position (ANOVA,  $P = 0.94$ ). The  
 592 mean  $F_{opt}$  for all positions was  $3.090 \pm 0.315$  Hz  
 593 (Fig. 6c). In addition to this, maximum oscillatory  
 594 power was the same for all positions on the brook  
 595 trout (ANOVA,  $P = 0.84$ ). The mean  $W_{max}$  for all  
 596 positions was  $11.735 \pm 1.091$  W kg $^{-1}$  (Fig. 6b).

597 In vitro workloop experiments using in vivo  
 598 muscle activity data were carried out for three  
 599 swimming speeds on bundles from each position  
 600 (Fig. 7). The shape of the workloops varies with  
 601 each position. There is an increase in work per  
 602 cycle, or the area of the workloop, from anterior  
 to posterior along the length of the fish. The



603

604 Fig. 5. Contraction kinetics of red muscle from brook trout at  
 605 10°C. Mean ( $\pm$ S.E.) values are given for each position ( $n = 4$ ).  
 606 Activation time (a) is the time from 10 to 90% of peak  
 607 isometric stress, relaxation time (b) from 90 to 10% of peak  
 608 isometric stress, and twitch time (c) from stimulation to 90%  
 609 recovery (or 10% of peak twitch stress remaining). There is no  
 610 significant affect of longitudinal position on any kinetic variable.



611 Fig. 6. Peak tetanic force, maximum oscillatory power ( $W_{max}$ )  
 612 and optimal oscillatory frequency ( $F_{opt}$ ) of brook trout red  
 613 muscle. Mean ( $\pm$ S.E.) values are given for each position  
 614 ( $n = 4$ ). Peak tetanic force (a) is determined from isometric  
 615 contraction.  $W_{max}$  (b) is found by optimizing the activity conditions  
 616 of the workloop experiments, and  $F_{opt}$  (c) is the oscillation  
 617 frequency at  $W_{max}$ . There was no significant variation in  
 618 peak force,  $W_{max}$  or  $F_{opt}$  along the length of the fish.

611

612

613

614

615

616

617

618

619

620 posterior region produces more work than the  
 621 anterior as indicated by the area of the workloop,  
 622 although the mean difference was relatively small.  
 623 The increase in the strain from anterior to posterior  
 624 across the length of the fish is demonstrated  
 625 by the increase in the width of the workloop.  
 626 When comparing workloops at one position for a  
 627 range of different swimming speeds, there was a  
 628 decrease in work per cycle with increasing speed.  
 629 For instance, the workloop for posterior muscle  
 630 at  $2.0$  BL s $^{-1}$  is slightly larger than the workloop  
 631 directly below it for  $4.0$  BL s $^{-1}$  (Fig. 7).

632 All the longitudinal positions produced about  
 633 the same amount of power at a given swimming  
 634 speed (Fig. 8). This was true for both observed  
 635 and long strains. While there was a general trend  
 636 for greater power output at posterior positions,  
 637 this was not statistically significant. (Multiway  
 638 ANOVAs,  $P = 0.295$  for observed strain,  $P =$   
 639  $0.248$  for long strain). When swimming speeds  
 640 were examined individually, no effect of position  
 641 on power output was found for any speed  
 642 (ANOVA,  $P > 0.15$  for all speeds). There was no  
 643 significant change in power output with increasing  
 644 in swimming speed (Multiway ANOVAs,  $P =$   
 $0.251$  for observed strain,  $P = 0.654$  for long

619

620

621

622

623

624

625

626

627

628

629

630

631

632

633

634

635

636

637

638

639

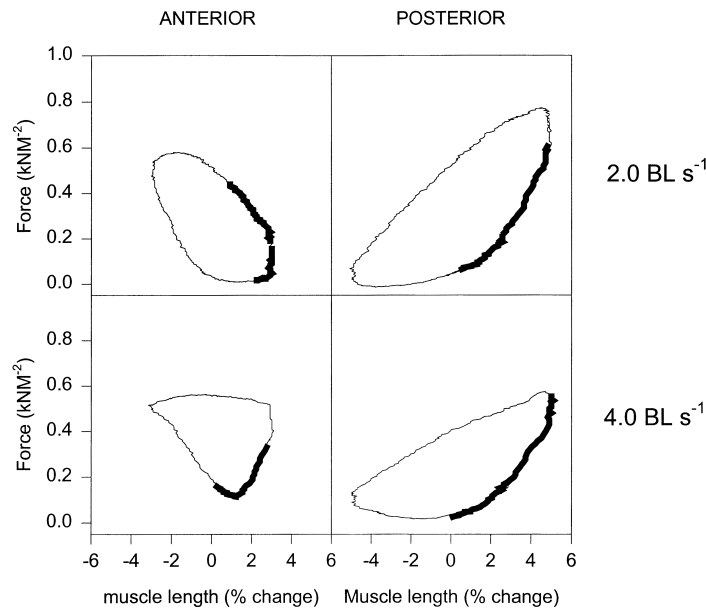
640

641

642

643

644

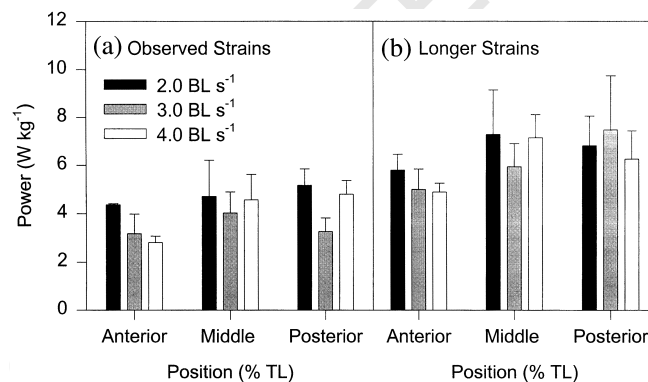


645 Fig. 7. Representative in vitro workloops for brook trout red muscle bundles at 10°C from the activity conditions found in vivo.  
 646 Positions on the fish are given across the top of the graph, and the representative swimming speeds are found to the right of the graph.  
 647 All work loops run in a counter clockwise direction. The bolding indicates stimulation. The area of the workloop gives the work output  
 648 per oscillatory cycle. The width of the workloop corresponds to the strain with the peak muscle length found at the right most extreme  
 649 of the workloop. Workloop force is normalized to maximal tetanic force. There was no statistically significant change in work per cycle  
 650 between swimming speeds, but there is an increase in work per cycle from anterior to posterior.

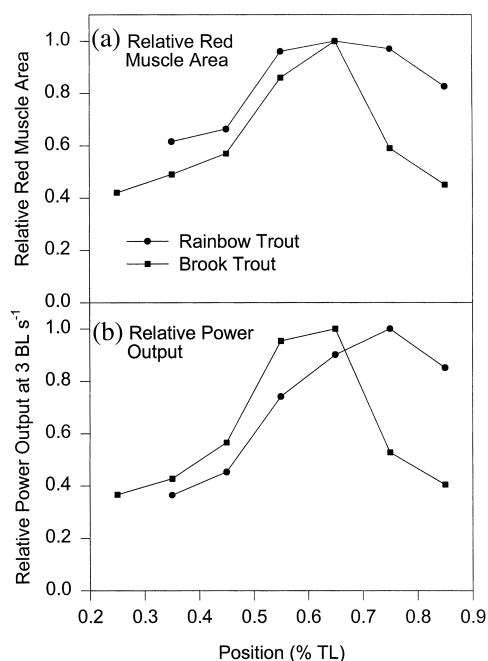
651 strain). The trend of work output per cycle to  
 652 decrease with increasing swimming speed was  
 653 balanced by the higher oscillation frequency at  
 654 higher speeds. This led to little change in mass-  
 655 specific power output across swimming speeds.

### 3.3. Distribution of red muscle and absolute power production

The patterns of red muscle area along the



661 Fig. 8. In vitro mass-specific power production by red muscle stimulated under in vivo muscle activity conditions (mean  $\pm$  S.E.). Power  
 662 output is plotted vs. position along the animal from which the muscle bundle and activity conditions were taken, at the three swimming  
 663 speeds. Power output is shown for the *observed* strains (a), those observed in brook trout, and for *long* strains (b), those observed in  
 664 rainbow trout. Long strains were used because the strains found in brook trout were relatively low in amplitude compared to rainbow  
 665 trout. There was no rostral-caudal variation in mass-specific power output for either observed or long strains. The results for the two  
 666 strain regimes are qualitatively the same, but longer strains simply resulted in more power. An increase in swimming speed also did not  
 667 affect the power output at a given position for observed or long strains.



668  
 669 Fig. 9. Relative muscle area (a) and relative power output (b)  
 670 in absolute terms for rainbow and brook trout. For both  
 671 variables, quantities are normalized. For both species, red or  
 672 slow muscle area and, therefore, mass was greatest at 0.65 TL.  
 673 When mass-specific power production was combined with the  
 674 mass of muscle at each position, the two species show differ-  
 675 ent rostral–caudal patterns of power production. No error  
 676 bars are given because the muscle areas presented are rela-  
 677 tively crude estimates of muscle area.

677  
 678 length of brook trout and rainbow trout were  
 679 similar, both showing a peak in muscle area at  
 680 0.65 TL, as previously reported for rainbow trout  
 681 (Ellerby et al., 2000). Differences in longitudinal  
 682 variations in mass-specific power output between  
 683 the two species were still observed when compar-  
 684 ing patterns of absolute power output. Expressed  
 685 in normalized terms, absolute power production  
 686 in brook trout peaks at the 0.55–0.65 TL posi-  
 687 tions, where muscle mass peaks (Fig. 9). In rain-  
 688 bow trout, power production peaks at 0.75 TL.  
 689 Although muscle mass is greater just in front of  
 690 this position, greater mass-specific power output  
 691 by posterior muscle results in higher absolute  
 692 power output at this position. The difference in  
 693 power production at 0.85 TL is even greater  
 694 between the two species (Fig. 9).

#### 695 696 4. Discussion 697

The function of red muscle during steady

698  
 699 swimming in brook trout seems to be different  
 700 than its role in same-sized rainbow trout and  
 701 several other previously studied species. Work-  
 702 loop estimates of mass-specific power output dur-  
 703 ing swimming, in ~20 cm rainbow trout, large-  
 704 mouth bass, and scup indicate that the posterior  
 705 region generates the majority of power during  
 706 steady swimming (Coughlin, 2000; Rome et al.,  
 707 2000). In at least rainbow trout and scup, the  
 708 rostral–caudal variation is even greater when  
 709 muscle area is included (Coughlin and Rome,  
 710 2000; this study). In 20-cm brook trout there is no  
 711 apparent difference in red mass-specific muscle  
 712 power output with any of the positions along the  
 713 fish for a given swimming speed. All positions  
 714 along the length of the red muscle of brook trout  
 715 generate approximately the same amount of  
 716 mass-specific power during steady swimming.  
 717 When muscle distribution is included, brook trout  
 718 produce the majority of power for swimming in  
 719 the middle regions, at the peak of muscle mass.

720  
 721 In rainbow trout, as well as large mouth bass  
 722 and scup, the activity pattern found in the red  
 723 anterior muscle acts as a constraint on mass-  
 724 specific power production when compared with  
 725 more posterior positions along the fish. Previous  
 726 studies found that the anterior muscle of these  
 727 and other fish species had the lowest strain during  
 728 swimming, the longest duty cycle and a smaller  
 729 phase shift of activation time relative to peak  
 730 muscle length. The reduction in power production  
 731 at the anterior region compared to the more  
 732 posterior positions is apparently due to longitudi-  
 733 nal variation in these muscle activity variables at  
 734 a given swimming speed (Coughlin, 2000). In the  
 735 case of scup, strain increases by >300%, and  
 736 duty cycle decreases by almost 50% from anterior  
 737 to posterior regions of the myotome (Rome et al.,  
 738 1993). Similar trends are seen in many fish species  
 739 (Altringham and Ellerby, 1999; Coughlin, 2000).  
 740 Alternatively, in brook trout variations in the red  
 741 muscle activity conditions during steady swimming  
 742 are relatively slight. For instance, strain increases  
 743 by only 50% from the anterior to posterior posi-  
 744 tion at most speeds. The change in duty cycle is  
 745 an approximate 10–15% decrease from anterior  
 746 to posterior. This is similar to red muscle activity  
 747 in mackerel (Shadwick et al., 1998) and adult  
 748 rainbow trout (Hammond et al., 1998). Shadwick  
 749 and colleagues suggested that power production  
 750 in mackerel would be a generalized feature of the  
 751 entire red myotome during steady swimming, as

750 did Hammond and colleagues for large rainbow  
751 trout. That same result is reported here brook  
752 trout. That same result is reported here brook  
753 trout.

754 In rainbow trout smolts, bass, scup and other  
755 species, contraction kinetics are affected by longi-  
756 tudinal position. In these fish, the anterior red  
757 muscle has a faster relaxation time than more  
758 posterior muscle (see Altringham and Ellerby,  
759 1999). In scup (Rome et al., 1993) and rainbow  
760 trout (Coughlin et al., in press), the posterior red  
761 muscle has a 100% longer relaxation than the  
762 anterior. Differences in kinetics do affect the  
763 power output of red muscle during steady  
764 swimming. Increased rates of relaxation benefit  
765 the anterior muscle more than the posterior mus-  
766 cle, allowing the anterior muscle to somewhat  
767 overcome the activation constraints mentioned  
768 above. The residual force in the muscle during  
769 the lengthening phase is greatly reduced with a  
770 faster relaxation time. Previous studies have  
771 shown that when both the anterior and posterior  
772 muscle are stimulated under less advantageous  
773 conditions specified by the anterior position, the  
774 faster anterior muscle produces more mass-  
775 specific power than the posterior (Rome et al.,  
776 1993; Coughlin, 2000). In brook trout activation  
777 time, relaxation time and twitch time were de-  
778 termined using the same methodology as previous  
779 work on scup, bass and rainbow trout but re-  
780 mained relatively constant along the length of the  
781 animal. For instance, the increase in relaxation  
782 time from anterior to posterior was only 40% and  
783 not statistically significant. In this species, the  
784 activity conditions of duty cycle, strain, and phase  
785 did not vary by position either. Since the muscle  
786 activity conditions do not vary greatly along the  
787 length of the swimming brook trout, there is  
788 apparently no benefit for rostral–caudal transfor-  
789 mations in muscle kinetics either.

790 Adult rainbow trout, which reportedly power  
791 steady swimming with their entire myotome as  
792 observed in brook trout, show reduced longitudi-  
793 nal variation in contraction kinetics compared to  
794 juveniles (Coughlin et al., in press). Large, adult  
795 rainbow trout display longitudinal variation in  
796 twitch time but not relaxation time (Hammond et  
797 al., 1998), while juvenile rainbow trout show lon-  
798 gitudinal variation in activation, relaxation and  
799 twitch time (Coughlin et al., in press). In adult  
800 trout, the activation conditions of red muscle  
801 along the length of the animal do vary during  
swimming. The similarities in patterns of contrac-

tion kinetics and power production between brook  
trout and adult rainbow trout suggest a point of  
departure for future work: are longitudinal pat-  
terns of red muscle contraction kinetics corre-  
lated with patterns of power production during  
steady swimming?

In brook trout, mass-specific power output did  
not significantly increase with swimming speed.  
This differs distinctly from previous work on scup  
(Rome et al., 2000), bass and rainbow trout smolts  
(Coughlin, 2000). This suggests that unlike these  
other species, faster swimming in brook trout  
would rely on increased recruitment of red mus-  
cle, not on increased power output by a given  
mass of red muscle.

The brook trout used in this study were ~ 20  
cm, the same size as rainbow trout smolts used in  
a previous study (Coughlin, 2000). Despite a close  
phylogenetic relationship and similarity in size,  
there are qualitative differences in the swimming  
of these two fish species. Patterns of power pro-  
duction by adult brook trout are comparable to  
those reported for much larger (~ 42 cm) adult  
rainbow trout and those predicted for mackerel  
(Shadwick et al., 1998). Why were strikingly dif-  
ferent results found between the ~ 20 cm brook  
trout and rainbow trout? Anatomically, the two  
species are quite similar in body form (although  
not in coloration). The two species have similar  
numbers of vertebrae, with 58–62 in brook trout  
(Scott and Crossman, 1973) and 61–65 in ‘coastal’  
strains of rainbow trout (as were used by Cough-  
lin, 2000) (Behnke, 1992). One clear difference  
between the two species is that there was a dra-  
matic shift in muscle kinetics from anterior to  
posterior in rainbow trout (Coughlin, 2000) but  
not in brook trout. In the brook trout, there was  
only a weak general trend towards slower kinetics  
in the posterior regions of the fish (Fig. 5). Dif-  
ferences in the longitudinal patterns of red mus-  
cle activity during steady swimming between these  
relatively closely related members of the family  
salmonidae and between different sizes of rain-  
bow trout suggest both evolutionary and develop-  
mental plasticity in the nervous control of muscle  
function and, ultimately, in red muscle’s role in  
powering steady swimming.

#### Uncited references

Jayne and Lauder, 1995

855 **Acknowledgements**

857 We thank James E. Harvey, Chief, Division of  
858 Trout Production of the Pennsylvania Fish and  
859 Boat Commission, and Paul Drumm, Manager,  
860 and David Jordan of the Huntsdale Fish Culture  
861 Station for supplying the experimental animals.  
862 This work was supported by an NSF-RUI Grant  
863 (Research at Undergraduate Institutions, IBN-  
864 9604140) and by grants from Widener University.  
865 We thank the NSF and Widener University for  
866 their generous support of undergraduate re-  
867 search.

869 **References**

872 Altringham, J.D., Johnston, I.A., 1990. Scaling effects  
873 on muscle function: power output of isolated fish  
874 muscle fibres performing oscillatory work. *J. Exp.*  
875 *Biol.* 151, 453–467.  
877 Altringham, J.D., Ellerby, D.J., 1999. Fish swimming:  
878 patterns in muscle function. *J. Exp. Biol.* 202,  
880 3397–3403.  
881 Behnke, R.J., 1992. Native Trout of Western North  
882 America. American Fisheries Society Monograph, p.  
883 6.  
885 Coughlin, D.J., 2000. Power production during steady  
886 swimming in largemouth bass and rainbow trout. *J.*  
887 *Exp. Biol.* 203, 617–629.  
889 Coughlin, D.J., Rome, L.C., 1996. The roles of pink and  
890 red muscle in powering steady swimming in scup,  
891 *Stenotomus chrysops*. *Am. Zool.* 36, 666–677.  
893 Coughlin, D.J., Rome, L.C., 1999. Muscle activity in  
894 steady swimming scup, *Stenotomus chrysops*, varies  
895 with fiber type and body position. *Biol. Bull.* 196,  
896 145–152.  
898 Coughlin, D.J., Burdick, J., Stauffer, K.A., Weaver, F.E.  
899 in press. Rainbow trout display a developmental shift  
900 in red muscle kinetics, swimming kinematics and  
901 myosin heavy chain isoform. *J. Fish Biol.*  
903 Ellerby, D.J., Altringham, J.D., Williams, T., Block,  
904 B.A., 2000. Slow muscle function of pacific bonito  
905 (*Sarda chiliensis*) during steady swimming. *J. Exp.*  
906 *Biol.* 203, 2001–2013.  
908 Gillis, G.B., 1998. Neuromuscular control of anguilli-  
909 form locomotion: patterns of red and white muscle  
910 activity during swimming in the American eel, *An-*  
911 *guilla rostrata*. *J. Exp. Biol.* 201, 3245–3256.

912 Hammond, L., Altringham, J.D., Wardle, C.S., 1998. 913  
Myotomal slow muscle function of rainbow trout 914  
*Oncorhynchus mykiss* during steady swimming. *J. Exp.* 915  
*Biol.* 201, 1659–1671. 916  
Jayne, B.C., Lauder, G.V., 1995. Red muscle motor 918  
patterns during steady swimming in largemouth bass: 919  
effects of speed and correlation with axial kinemat- 920  
ics. *J. Exp. Biol.* 198, 657–670. 922  
Josephson, R.K., 1985. Mechanical power output from 923  
striated muscle during cyclical contraction. *J. Exp.* 924  
*Biol.* 114, 493–512. 926  
Rome, L.C., Swank, D., Corda, D., 1993. How fish 927  
power swimming. *Science* 261, 340–343. 928  
Rome, L.C., Swank, D.M., Coughlin, D.J., 2000. The 930  
influence of temperature on power production dur- 931  
ing swimming II. Mechanics of red muscle fibres in 932  
vivo. *J. Exp. Biol.* 203, 333–345. 934  
Scott, W.B., Crossman, E.J., 1973. Freshwater Fishes of 935  
Canada. Bryant Press, Limited, Canada. 936  
Shadwick, R.E., Steffensen, J.F., Katz, S.L., Knower, T., 938  
1998. Muscle dynamics in fish during steady 939  
swimming. *Am. Zool.* 38, 755–770. 940  
Shadwick, R.E., Katz, S.L., Kormsmeier, K.E., Knower, 942  
T., Covell, J.W., 1999. Muscle dynamics in skipjack 943  
tuna: timing of red muscle shortening in relation to 944  
activation and body curvature during steady 945  
swimming. *J. Exp. Biol.* 202, 2139–2150. 946  
Swank, D.M., Rome, L.C., 2000. The influence of tem- 948  
perature on power production during swimming I. In 949  
vivo length change and stimulation patterns. *J. Exp.* 950  
*Biol.* 203, 321–331. 952  
van Leeuwen, J.L., 1995. The action of muscles in 953  
swimming fish. *Exp. Physiol.* 80, 177–191. 954  
van Leeuwen, J.L., Lankheet, M.J.M., Akster, H.A., 956  
Osse, J.W.M., 1990. Function of red axial muscles of 957  
carp (*Cyprinus carpio*): recruitment and normalized 958  
power output during swimming in different modes. *J.* 959  
*Zool. Lond.* 220, 123–145. 960  
Wardle, C.S., Videler, J.J., 1993. The timing of the 962  
electromyogram in the lateral myotomes of mackerel 963  
and saithe at different swimming speeds. *J. Fish Biol.* 964  
43, 347–359. 966  
Wardle, C.S., Videler, J.J., Altringham, J.D., 1995. Tun- 967  
ing in to fish swimming waves: body form, swimming 968  
mode and muscle function. *J. Exp. Biol.* 198, 969  
1629–1636. 970  
Zhang, G., Swank, D.M., Rome, L.C., 1996. Quantita- 972  
tive distribution of muscle fiber types in the scup. *J.* 973  
*Morph.* 229, 71–81.